
Tumor-Specific In Vivo Transfection with HSV-1 Thymidine Kinase Gene Using a Sindbis Viral Vector as a Basis for Prodrug Ganciclovir Activation and PET

Jen-Chieh Tseng¹, Pat B. Zanzonico², Brandi Levin¹, Ronald Finn³, Steven M. Larson⁴, and Daniel Meruelo¹

¹*NYU Cancer Institute, Rita J. and Stanley H. Kaplan Comprehensive Cancer Center, and NYU Gene Therapy Center, NYU School of Medicine, New York, New York;* ²*Department of Medical Physics, Memorial Sloan-Kettering Cancer Center, New York, New York;* ³*Cyclotron and Radiochemistry Facility, Department of Radiology, Memorial Sloan-Kettering Cancer Center, New York, New York;* and ⁴*Nuclear Medicine Service, Department of Radiology, Memorial Sloan-Kettering Cancer Center, New York, New York*

One type of gene therapy of tumors, gene-directed enzyme-prodrug therapy (GDEPT), holds considerable promise, although practical considerations limit its clinical applicability. These include the lack of acceptable noninvasive methods that are adaptable to humans for selective tumor targeting of the therapeutic genetic material. Sindbis virus is an oncolytic, α -virus that selectively targets tumors through the 67-kDa laminin receptor (LAMR). In this report we describe a novel approach that permits tumor-selective tumor targeting and quantitative in vivo monitoring using PET of a commonly applied GDEPT, based on herpes simplex virus thymidine kinase type 1 (HSVtk) and ganciclovir (GCV). **Methods:** Sindbis/tk vectors were harvested from the supernatant of in vitro cultures of a packaging cell produced by electroporation of both replicon RNA (SinRep5/tk) and helper RNA (DH-BB) into baby hamster kidney (BHK) cells. The therapeutic effect of GCV was determined by incubation of transfected tumor cells with increasing concentrations of GCV. BHK tumors growing as xenografts in severe combined immunodeficiency disease (SCID) mice were transfected by parenteral administration of the vector. Imaging was performed using small-animal PET at 2 h after injection of ¹⁸F fluoro-ethyl-arabinosyluridine (¹⁸F-FEAU) and 24 h after the final parenteral injection of Sindbis/tk viral vector. **Results:** The vector efficiently expresses the HSVtk enzyme in infected tumor cells, both in vitro and in vivo. High levels of HSVtk expression ensure sufficient prodrug GCV conversion and activation for bystander effects that kill the surrounding untransduced tumor cells. Tumor localization of intravenously administered ¹⁸F-FEAU after 2 and 3 parenteral vector treatments of Sindbis/tk demonstrated uptake of 1.7 and 3.1 %ID/g (percentage injected dose per gram), respectively. **Conclusion:** The vector efficiently targets the HSVtk enzyme gene into Sindbis-infected tumor cells. High levels of HSVtk expression ensure sufficient prodrug GCV conversion and activation for bystander effects that killed many surrounding untransduced tumor cells. In addition, the HSVtk activities in tu-

mors can be noninvasively monitored using PET after systemic Sindbis/tk treatments as a basis for determining the levels and tissue distribution of vector, noninvasively in living animals, and for optimizing in vivo transfection rates of tumor.

Key Words: Sindbis vector; herpes simplex virus thymidine kinase type 1; gene-directed enzyme-prodrug therapy; PET; in vivo imaging

J Nucl Med 2006; 47:1136–1143

Gene therapy targets the genome of tumor cells as a basis for a highly selective and nontoxic anticancer therapy. To enhance selectivity and specificity to the killing of cancer cells, several enzyme/prodrug systems—such as carboxylesterase/CPT-11 (1), cytosine deaminase/5-fluorocytosine (2), and herpes simplex virus thymidine kinase type 1 (HSVtk)/ganciclovir (GCV) (3,4)—have been developed for gene-directed enzyme-prodrug therapy (GDEPT). In this strategy, tumor cells are transduced with therapeutic genes that encode enzymes for specific conversion/activation of prodrugs, which are toxicologically inert at relatively high doses, into highly toxic metabolites for tumor killing.

Clinically successful GDEPT will require not only an appropriate enzyme/prodrug combination but also a gene therapy vector by which the gene encoding the enzyme can be delivered efficiently and specifically to tumors (5). In addition, it would be ideal for such vectors to target tumors systemically for the treatment of advanced metastatic diseases. Several viral gene therapy vectors have been tested for GDEPT with different enzyme/prodrug combinations. However, the relatively poor responses observed in preclinical and clinical studies using vectors based on adenoviruses or retroviruses could be largely due to insufficient gene transfer and inefficient gene expression within tumors. We recently discovered that vectors based on

Received Nov. 16, 2005; revision accepted Mar. 22, 2006.
For correspondence contact: Daniel Meruelo, PhD, Department of Pathology, NYU School of Medicine, 550 First Ave., New York, NY 10016.
E-mail: merued01@med.nyu.edu
COPYRIGHT © 2006 by the Society of Nuclear Medicine, Inc.

Sindbis virus, a blood-borne alphavirus transmitted through mosquito bites, infect tumor cells specifically and systemically throughout the body (6,7). The tumor specificity of Sindbis vectors may be mediated by the 67-kDa high-affinity laminin receptor (LAMR) (8), which is overexpressed in several types of human tumors (9–12). Another advantageous property of Sindbis vectors for cancer therapy is that, without carrying cytotoxic genes, they have been shown to induce apoptosis in mammalian cells (13–15). Furthermore, as Sindbis vectors are capable of expressing very high levels of their transduced suicide genes in infected tumor cells, the efficient production of the enzymes for sufficient prodrug conversion is ensured.

One of the best-studied enzyme/prodrug systems for cancer GDEPT is the HSVtk/GCV system (3). GCV, which has been clinically approved for the treatment of HSV and cytomegalovirus infections in humans, is a poor substrate for the mammalian nucleoside monophosphate kinase but can be converted efficiently (~1,000-fold more) into the monophosphate by herpes viral thymidine kinase. Subsequent phosphorylation of the monophosphate performed by cellular enzymes leads to the generation of GCV triphosphate, which competes with deoxyguanosine triphosphate for incorporation into elongating DNA during the S phase of the cell cycle. GCV incorporation inhibits the DNA polymerase and induces single-strand breaks eventually leading to cell death (16). This feature makes the HSVtk/GCV system suitable for eradicating rapidly dividing tumor cells while sparing nonproliferating normal tissues. Several studies have suggested that the HSVtk/GCV GDEPT kills tumor cells via apoptotic pathways (17,18), although the mechanism is still unclear. A bystander effect that can play an important role in the eradication of surrounding untransduced tumor cells is caused by transmission of the activated prodrug from the transduced tumor cells, which may be only a small fraction of total tumor mass. In the HSVtk/GCV system, the activated GCV is not membrane permeable because of its highly charged phosphate groups. However, it can be transferred via the gap junctions or through the exchange of apoptotic vesicles that kill the surrounding untransduced tumor cells (19).

To enhance the efficacy of prodrug activation and to reduce the possible toxicity caused by systemic prodrug treatment, the ability to monitor the levels of suicide gene expression in patients after administering the gene therapy vectors would significantly improve GDEPT. PET is a powerful tool because the imaging can be readily translated across the spectrum from mouse to human. Such imaging information could help optimize the dosing and timing of GDEPT treatments and thus minimize or prevent toxicity of the prodrugs. Several PET tracers, including ^{124}I -FIAU (2'-fluoro-2'-deoxy-1- β -D-arabinofuranosyl-5-iodo-uracil) and ^{18}F -FEAU (2'-fluoro-2'-deoxy-1- β -D-arabinofuranosyl-5-ethyl-uracil) have already been developed for monitoring HSVtk activity in living subjects (20–23), thus enabling us to follow the therapeutic outcomes of the HSVtk/GCV GDEPT.

In this report we demonstrate that a GDEPT vector based on Sindbis virus, Sindbis/tk, can successfully deliver the HSVtk suicide gene to tumor cells for subsequent GCV activation and tumor killing. In addition, we demonstrate the utility of PET to monitor the HSVtk activity in tumor cells after parenteral administration of Sindbis/tk vector. Our data indicate that Sindbis vectors are promising GDEPT agents not only for tumor detection but also for therapeutic evaluation after HSVtk/GCV GDEPT.

MATERIALS AND METHODS

Cell Lines and Vector Production

Baby hamster kidney (BHK) and ES-2 cells were obtained from the American Type Culture Collection. BHK cells were maintained in minimum essential α -modified media (α MEM, JRH Bioscience) with 5% fetal bovine serum (FBS). ES-2 cells were cultured in McCoy's 5A medium (Mediatech, Inc.) supplemented with 10% FBS. To express firefly luciferase (Fluc) for noninvasive bioluminescent imaging, we derived ES-2/Fluc cells from the ES-2 line by stable transfection of a plasmid, pIRES2-Fluc/EGFP, as described (7). All basal media were supplemented with 100 $\mu\text{g}/\text{mL}$ of penicillin–streptomycin (Mediatech) and 0.5 $\mu\text{g}/\text{mL}$ of amphotericin B (Mediatech).

Sindbis vectors were produced by electroporation of both replicon RNA (SinRep5) and helper RNA (DH-BB) into BHK cells as described (6). The HSV-1 thymidine kinase (HSVtk) gene was excised from the pORF-HSV1tk plasmid (InvivoGen Co.) and inserted into the *Pml*I site of the SinRep5 plasmid (Invitrogen) for Sindbis/tk vector production. A similar procedure was performed to generate the Sindbis/gfp vector, which carries an enhanced green fluorescent protein gene obtained from the pEGFP-N1 plasmid (BD Biosciences Clontech). Sindbis/lacZ vectors were produced using a pSinRep5/lacZ (Invitrogen) plasmid as described (6).

Western Blot

We infected 2×10^5 BHK cells with Sindbis/tk or Sindbis/lacZ at a multiplicity of infection (MOI; transducing units [TU]/cell number) of 50 as described (6). The next day, cells were lysed on ice with 500 μL of RIPA (radioimmunoprecipitation assay) lysis buffer (150 mmol/L NaCl, 1% Nonidet P-40, 50 mmol/L Tris-HCl, pH 8, 0.5% sodium deoxycholate, and 0.1% sodium dodecyl sulfate [SDS]) and 15 μL of lysate supernatant were separated on 12% SDS-polyacrylamide gel electrophoresis (PAGE) under denaturing condition. We used a polyclonal rabbit anti-HSVtk antibody (1:100 dilution; Dr. William C. Summers, Yale University, New Haven, CT) to detect the presence of HSVtk enzyme. The antibody-HSVtk complexes were later stained with a donkey antirabbit IgG conjugated with alkaline phosphatase (1:7,500 dilution; Pierce Biotechnology Inc.). The lower-molecular-weight band might have resulted from partial degradation that was detected by the polyclonal anti-HSVtk antibody.

Thymidine Kinase Activity Assay

We infected 1×10^6 of BHK or ES-2/Fluc cells with Sindbis/tk vectors at MOI = 10. For comparison, uninfected cells were included as controls. The day after infection, cells were lysed with 1 mL of M-PER lysis buffer (Pierce Biotechnology) at room temperature for 5 min. The cell lysates were centrifuged, and 10 μL of supernatants (containing ~20 μg of protein) were analyzed for thymidine kinase activity. The assays were performed at 37°C

for 1 h in 200 μ L reaction buffer containing 50 mmol/L Tris-HCl, 10 mmol/L $MgCl_2$, 10 mmol/L adenosine triphosphate, and 10 μ L of methyl- 3H -thymidine solution (200 μ mol/L; 37 MBq/mL [1 mCi/mL]; specificity, 185 GBq/mmol [5 Ci/mmol]; Amersham Biosciences Inc.). reactions that contain no cell lysates were also performed. To stop the reaction, the reactions were incubated at 95°C for 3 min and then loaded onto DE81 filters (Whatman Inc.). The filters were washed 2 times with 2 mL of 4 mmol/L NH_4COOH and 3 times with 5 mL of ethanol. After drying under a heat lamp, the activity on the filters was measured in a scintillation counter. Duplicate results were reported for infected BHK cells and triplicate results were reported for infected ES-2/Fluc cells.

Cytotoxicity Assay

On day 0, 1.5×10^5 ES-2/Fluc cells were infected with Sindbis/tk or Sindbis/gfp at MOI = 10 and cultured in the presence of GCV (0–50 μ g/mL GCV sodium, CYTOVENE-IV; Roche Laboratories Inc.). Uninfected cells (control) were included for comparison. On day 2, surviving cells were analyzed using a CellTiter 96 AQueous nonradioactive cell proliferation assay kit [MTS [3-(4,5-dimethylthiazol-2-yl)-5-(3-carboxymethoxyphenyl)-2-(4-sulfophenyl)-2H-tetrazolium, inner salt]; Promega U.S.). The cells were cultured at 37°C for 1.5 h in 0.6 mL of McCoy's 5A medium containing 0.1 mL of MTS solution and 5 μ L of PMS solution. For each sample, 100 μ L of reaction medium were transferred onto a 96-well enzyme-linked immunosorbent assay plate and the colorimetric signal was determined at A_{490} . For each treatment group (Sindbis/tk, Sindbis/gfp, or control), we determined the relative growth using the A_{490} reading of cells cultured in 0 μ g/mL GCV to normalize each data point, which represented 3 independent assays.

IVIS Imaging

All animal experiments were performed in accordance with National Institutes of Health and institutional guidelines. C.B-17-SCID (severe combined immunodeficiency disease) mice (female, 6- to 8-wk old; Taconic) were injected intraperitoneally with 2×10^6 ES-2/Fluc cells in 0.5 mL McCoy's 5A medium on day 0. We initiated the daily intraperitoneal GDEPT treatments of Sindbis/tk ($\sim 10^7$ TU) or GCV (25 mg/kg of body weight) on day 3. The bioluminescence signals were monitored using the IVIS system 100 (Xenogen Corp.) on days 1, 3, 6, 8, 12, and 14. Before imaging, each mouse was injected intraperitoneally with 0.3 mL of luciferin (15 mg/mL potassium salt; Promega Corp.) in phosphate-buffered saline. After 5 min, mice were anesthetized with 0.3 mL of Avertin (1.25% of 2,2,2-tribromoethanol in 5% *t*-amyl alcohol). An integration time of 30 s was used for high-resolution (binning = 2) luminescent imaging. Living Image software (version 2.11; Xenogen Corp.) was used to analyze the bioluminescence signals (in terms of photons/cm²/s/steradian) from the animals.

^{14}C -FIAU Uptake Experiment

Two million ES-2/Fluc cells were either uninfected (control) or infected with Sindbis/tk at MOI = 5. The next day, cells were cultured in 10 mL of McCoy's 5A/FBS medium containing 3.7 kBq (0.1 μ Ci) of ^{14}C -FIAU. After 1, 2, 4, 6, or 24 h of incubation, a liquid scintillation counter was used to assay the radioactivity in the medium and in the cell pellets. Percentage uptakes of ^{14}C -FIAU in cells were determined using the formula: (net counts in cell pellet)/(net counts in cell pellet + net counts in medium) $\times 100\%$.

Preparation of PET Radiotracer ^{18}F -FEAU

Aqueous ^{18}F -fluoride was produced using a cyclotron (model R019/9; Ebc Technologies, Inc.) via the $^{20}Ne(d,\alpha)^{18}F$. ^{18}F was added to a solution of *n*-Bu₄NHCO₃ (50 μ L, 4% by weight) in a vial and evaporated azeotropically with anhydrous acetonitrile (2 \times 1 mL) at 80°C under a stream of dry nitrogen. A solution of 2-*O*-(trifluoromethylsulfonyl)-1-3-5-tri-*O*-benzyl- α -D-ribofuranose (5–6 mg in 0.5 mL anhydrous acetonitrile) was added to the dry residue, and the reaction mixture was heated at 80°C–82°C for 30 min. After cooling, the reaction mixture was passed through a silica SepPak column and eluted with 2.5 mL of ethyl acetate. The solution was evaporated to dryness at 80°C under a stream of dry nitrogen, and the residue was dissolved in 0.4 mL dichloroethane under dry nitrogen followed by the addition of 0.1 mL 30% HBr in AcOH. The reaction mixture was heated at 80°C–82°C for 10 min, 1 mL of toluene was added to the reaction mixture, and the HBr/AcOH was evaporated under a stream of dry nitrogen. A freshly prepared solution of 2,4-bis-*O*-trimethylsilyl-5-ethyl-uracil in dichloroethane (75–85 μ mol in 0.5 mL) was added to the residue, and the reaction mixture heated at 97°C–100°C for 60 min. The reaction mixture was cooled, passed through a silica SepPak column, and eluted with 2.5 mL 10% MeOH in dichloromethane. After evaporation of the solvent, the reaction mixture was heated to reflux with 0.3 mL of 0.1 mol/L sodium methoxide in methanol and then cooled and neutralized with 0.15 mL of 2 mol/L HCl in MeOH. The crude product was injected into a C₁₈ high-performance liquid chromatography column (10 \times 250 mm) and eluted with 10% acetonitrile in water at a flow of 4.05 mL/min. The product fraction was collected, evaporated to dryness, reconstituted in saline, and filtered through a 0.22- μ m sterile filter.

PET Studies

BHK cells (4×10^6) were injected subcutaneously in the right shoulders of NOD-SCID mice (NOD.CB17-Prkdc^{scid}/J, 6- to 8-wk old, female; The Jackson Laboratory) on day 0. The mice were randomly assigned to untreated control ($n = 5$) and Sindbis/tk groups ($n = 5$). Our previous observation (7) indicated that the BHK subcutaneous tumor model required multiple treatments to reach its maximal expression level. Therefore, on days 10, 11, and 13, the Sindbis/tk group received intraperitoneal treatments, consisting of 0.5 mL of Opti-MEM I containing 10^7 – 10^8 colony-forming units (CFU) of Sindbis/tk vectors, in the left flank of the lower abdomen consisting of 0.5 mL of Opti-MEM I containing 10^7 – 10^8 CFU of Sindbis/tk vectors. Control mice received no treatments. For PET on day 12 (first imaging) and day 14 (second imaging), mice were injected with at least 3.7 MBq (0.1 mCi) of ^{18}F -FEAU via the tail vein. Two hours later, the mice were anesthetized with isoflurane (Baxter Healthcare) and imaged in the R4 microPET (Concorde Microsystems Inc.), a dedicated 3-dimensional small-animal PET scanner (24). An energy window of 350–750 keV and a coincidence timing window of 6 ns were used, with a minimum of ~ 20 million events, typically acquired over ~ 5 min. The resulting list-mode data were sorted into 2-dimensional histograms by Fourier rebinning, and transverse images were reconstructed by filtered backprojection into a 128 \times 128 \times 63 (0.72 \times 0.72 \times 1.3 mm) matrix. The reconstructed spatial resolution for ^{18}F is 2.2-mm full width half maximum (FWHM) at the center of the field of view to 3.2-mm FWHM offset 5 cm from the center of the field of view. The image data were corrected for nonuniformity of response of the

microPET (i.e., were normalized), dead-time count losses, and physical decay to the time of injection but no attenuation, scatter, or partial-volume averaging correction was applied. An empirically determined system calibration factor (i.e., $\mu\text{Ci/mL/cps/voxel}$) for mice was used to convert voxel counting rates to activity concentrations, and the resulting image data were then normalized to the administered activity to determine by region-of-interest analysis the maximum %ID/g (percentage of injected dose per gram of tumor corrected for radioactive decay to the time of injection) in the tumors.

Statistical Analysis

We performed standard Student *t* tests (2-tail) and 2-way ANOVA analyses using GraphPad Prism version 3.0a for Macintosh (GraphPad Software). The error bars represent the SEM.

RESULTS

Sindbis/tk Efficiently Transduces HSVtk Activity in Infected Tumor Cells

For HSVtk/GCV GDEPT, we generated a Sindbis viral vector, Sindbis/tk, that carries an HSVtk complementary DNA sequence. The HSVtk expression is driven by the Sindbis viral subgenomic promoter that ensures a high level of expression after vector infection. Western blot analysis confirmed the expression of HSVtk (~46 kDa) in Sindbis/tk-infected baby hamster kidney (BHK) cells (Fig. 1A). No HSVtk was detected in BHK cells infected with a control Sindbis/lacZ vector that carries a bacterial β -galactosidase gene. In addition, we observed high levels of thymidine kinase activity, as determined by a ^3H -thymidine incorporation assay, in Sindbis/tk-infected BHK and human ES-2 clear cell ovarian carcinoma cells (Fig. 1B).

Transduced HSVtk Activity in Tumor Cells Enhances Antitumor Efficacy of Sindbis Vector in Presence of GCV

Efficient HSVtk transduction and expression in tumor cells should facilitate the activation of GCV and, therefore, enhance the bystander effect and tumor killing. We first determined the enhanced cytotoxicity induced by GCV in cultured ES-2/Fluc cells infected with Sindbis/tk vectors. ES-2/Fluc cells were derived from ES-2 cells that were stably transduced to express firefly luciferase (Fluc) for noninvasive bioluminescent imaging (25). ES-2/Fluc cells were infected with Sindbis/tk or Sindbis/gfp that carries an enhanced green fluorescent protein gene. After infection, cells were cultured in different concentrations of GCV. Two days after infection, we used the MTS respiratory assay to determine their relative growth compared with infected cells cultured without GCV. Similar to a previous *in vitro* observation (26), GCV significantly enhanced the cytotoxicity of Sindbis/tk vectors compared with control Sindbis/gfp vectors ($P = 0.0139$, 2-way ANOVA; Fig. 2A). No significant effects of GCV treatments were observed between uninfected (control) and Sindbis/gfp-infected cells, suggesting that the drug had no effect on Sindbis infection.

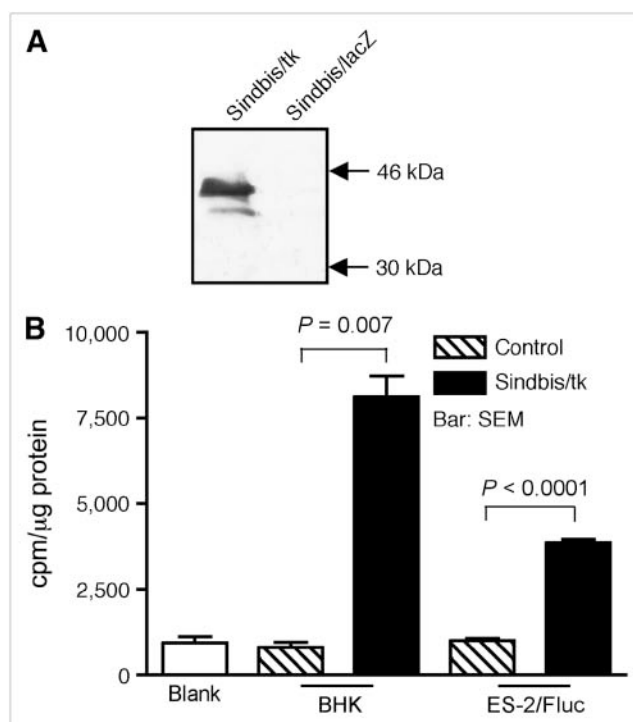


FIGURE 1. Sindbis/tk vector efficiently transduces HSVtk activity to infected cells. (A) Western blot analysis of HSVtk expression. Cell lysates from BHK cells infected with Sindbis/tk, which carries HSV-1 thymidine kinase gene, or with Sindbis/lacZ, which carries bacterial β -galactosidase gene, were separated on 12% SDS-PAGE before probing with a polyclonal antibody specific for HSVtk. Specific ~46-kDa band corresponding to HSVtk was observed in Sindbis/tk-infected cells but not in Sindbis/lacZ-infected cells. (B) Thymidine kinase activities in cell lysates from BHK ($n = 2$) or ES-2 ($n = 3$) cells infected with Sindbis/tk. Blank assays contained no cell lysate in reaction mixtures. BHK control ($n = 2$) and ES-2 control ($n = 3$) assays used lysates from cells that were not infected with Sindbis/tk.

GCV Enhances Antitumor Activity of Sindbis/tk Vector In Vivo

We later tested the Sindbis/tk GDEPT system *in vivo* using the previously established ovarian cancer model induced by intraperitoneal inoculation of ES-2/Fluc cells in SCID mice (7). The disease progression and the responses to Sindbis/tk GDEPT can be quantitatively monitored by the IVIS optical imaging system. Our previous data demonstrated that Sindbis vectors systemically targeted tumor metastases in the peritoneal cavity (25). On day 0, mice were inoculated intraperitoneally with 2×10^6 ES-2/Fluc cells and were imaged using the IVIS system 100 on day 1. We initiated the daily GDEPT intraperitoneal treatments with Sindbis/tk ($\sim 10^7$ TU) on day 3. Starting on day 4, Sindbis/tk-treated mice were treated daily with or without GCV (25 mg/kg of body weight, intraperitoneal injection) for prodrug administration. The disease progression was monitored by IVIS imaging on days 6, 8, 12, and 14. For comparison, mice that received no Sindbis/tk treatments (control) were treated with or without GCV to

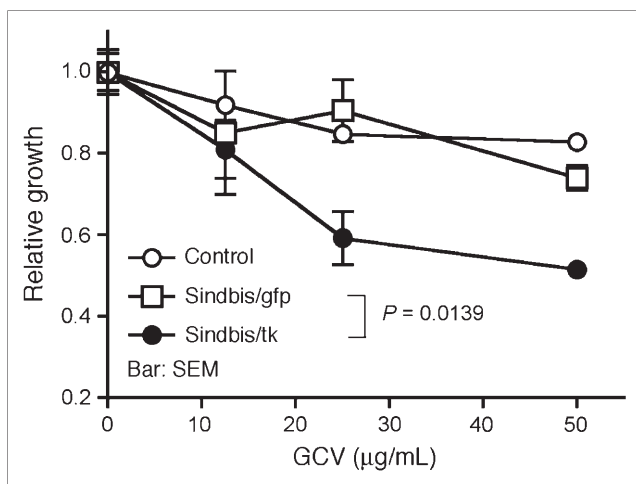


FIGURE 2. GCV, a prodrug activated by HSVtk, specifically enhances the cytotoxicity of Sindbis/tk vector against tumor cells. GCV enhances killing of Sindbis/tk-infected ES-2/Fluc cells in vitro, as determined by MTS respiratory assay. ES-2/Fluc cells, which stably express firefly luciferase gene, were left uninfected (control) or infected with Sindbis/tk vector Sindbis/gfp carrying a green fluorescent protein gene. After infection, cells were cultured for 2 d in medium containing different concentrations of GCV (0–50 µg/mL). Relative cell growth was determined using MTS assay that measures respiration of survived cells. Error bars represent SEM of triplicate data.

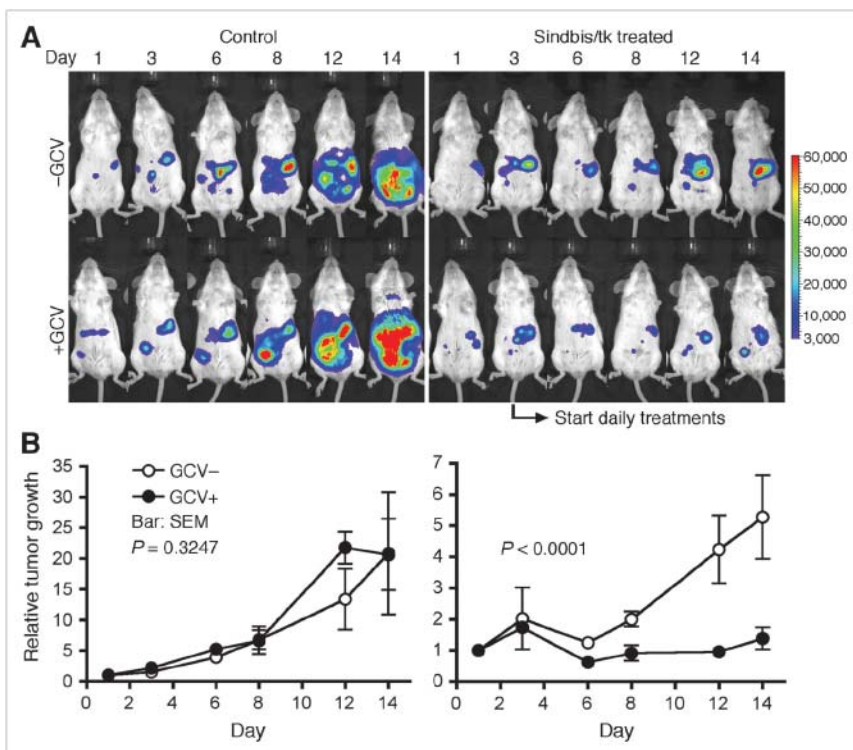
determine the baseline toxicity of GCV to ES-2/Fluc tumors. As shown in Figure 3A, the GCV treatments alone had no effect on tumor growth ($P = 0.3247$, 2-way ANOVA; Fig. 3B). However, the bystander effects of GCV signifi-

cantly enhanced the therapeutic responses to Sindbis/tk treatments ($P < 0.0001$, 2-way ANOVA).

Specific Tumor Targeting of Sindbis/tk Vector Determined by PET

Sindbis vectors carrying bioluminescent genetic markers are capable of detecting subcutaneous tumors or tumor metastases in small laboratory animals (7,25). Beside systemic detection, the vector can suppress their growth. However, because of the very limited penetrability of visible light, bioluminescent imaging technologies are not likely to be suitable for tumor detection in clinical settings. On the other hand, PET may provide an attractive alternative for determining the delivery efficiency of gene therapy vectors. Several fluorinated analogs of GCV have been developed as PET tracers for HSVtk detection in vivo, including radio-labeled FIAU (21,23) and FEAU (22). Once taken up by HSVtk-transduced tumor cells, the tracers are phosphorylated and accumulate within the tumor cells. We first determined whether Sindbis/tk-infected tumor cells were capable of efficient accumulation of the ^{14}C -FIAU in vitro. As shown in Figure 4, ES-2/Fluc cells transduced with Sindbis/tk vectors concentrated the ^{14}C -FIAU tracers specifically and efficiently within 8 h after infection. Conversely, only very low tracer accumulation was observed in uninfected control cells (~200 times less compared with infected cells). We subsequently used PET to detect the HSVtk enzyme activity in tumors transduced with Sindbis/tk vectors. SCID mice bearing subcutaneous BHK tumors on the shoulders received intraperitoneal Sindbis/tk treatments that enable systemic vector delivery for tumor

FIGURE 3. GCV enhances killing of Sindbis/tk-infected ES-2/Fluc cells in vivo, as determined by the IVIS system capable of noninvasive detection of bioluminescent signal generated by ES-2/Fluc tumors. (A) SCID mice were inoculated with ES-2/Fluc on day 0. We started daily GDEPT treatments composed of Sindbis/tk (~ 10^7 TU) and GCV (25 mg/kg of body weight) on day 3 (indicated by arrow). Sindbis/tk -GCV group ($n = 5$) received Sindbis/tk treatments but no GCV. Sindbis/tk +GCV group ($n = 5$) received both Sindbis/tk and GCV treatments. Control -GCV group ($n = 5$) was treated neither with Sindbis/tk nor with GCV. Control +GCV group ($n = 5$) received no Sindbis/tk but was treated with GCV. Disease progression was monitored and whole-body photon counts were determined using the IVIS system on days 1, 3, 6, 8, 12, and 14. Representative images of each treatment group are shown. (B) Quantitative presentations (total-body photon counts) of each treatment group as shown in A.



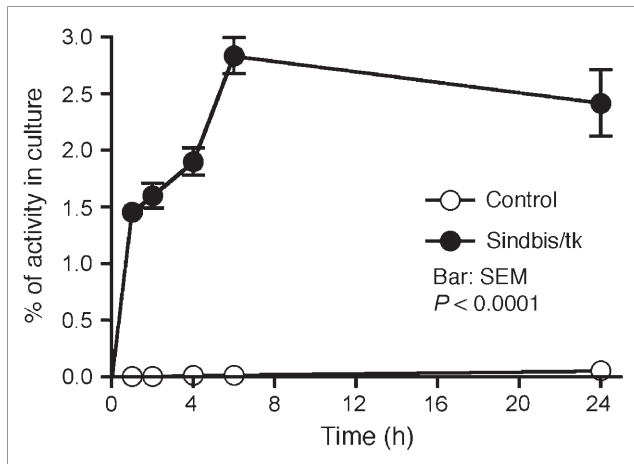


FIGURE 4. Sindbis/tk-infected ES-2/Fluc cells took up the HSVtk tracer, ^{14}C -FIAU, specifically and efficiently compared with uninfected control cells. Specific uptakes in cells were determined by a scintillation counter and are presented as percentage cellular uptakes of total radioactivity added into culture.

targeting (6,7). The tumors were inoculated on day 0 and the mice were treated with Sindbis vectors on day 10, 11, and 13. Because the tumors were inoculated on the shoulders, the vectors were administered remote from the tumor inoculation sites. On day 12 and 14, we determined tumor-specific HSVtk activity using microPET with the tracer ^{18}F -FEAU (Fig. 5). There was no significant change in tumors that received no Sindbis treatments. Radiotracer concentra-

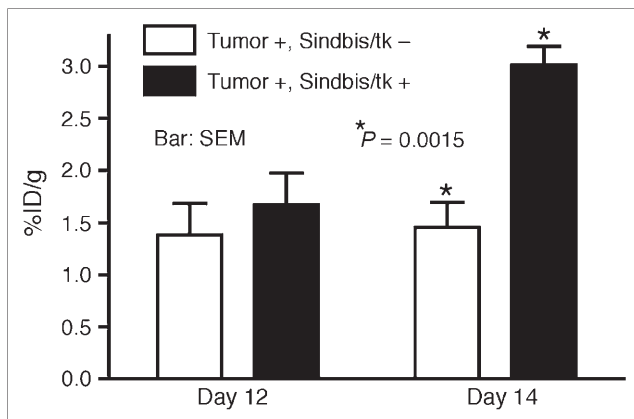


FIGURE 5. Quantitative analysis of HSVtk activity in subcutaneous tumors on SCID mice using microPET. BHK subcutaneous tumors were inoculated on right shoulders of SCID mice on day 0. On days 10, 11, and 13, mice received intraperitoneal treatments of Sindbis/tk vectors. Sites of vector treatments were far away from tumor inoculation sites. Untreated tumor-bearing mice were also included as imaging control. Tumor-specific HSVtk activities were measured on days 12 and 14 using ^{18}F -FEAU as tracer. Maximum pixel intensity (%ID/g) in tumor region of each untreated animal (Tumor +, Sindbis/tk -; $n = 5$) and Sindbis/tk-treated animal (Tumor +, Sindbis/tk +; $n = 5$) was calculated and analyzed using Student t test ($P = 0.0015$).

tions in tumors increased from 1.7 to 3.1 %ID/g after 2 (day 12) and 3 (day 14) treatments, respectively. The gradual increase of transgene activity in subcutaneous tumors is in accordance with our previous observation (7). In addition, after 3 treatments, PET clearly demonstrated higher ^{18}F -FEAU activity concentration in, and therefore successful systemic targeting to, these tumors (Tumor +, Sindbis/tk +; Fig. 6). The PET image intensity was lower in tumors in tumor-bearing mice that received no Sindbis/tk treatments (Tumor +, Sindbis/tk -; Fig. 6). Quantitative analysis of the PET image indicated that at 2 h after injection, the ^{18}F -FEAU activity concentration in the Sindbis/tk-treated tumor, 3.1 ± 0.18 %ID/g (mean \pm SEM), was significantly higher than that, 1.5 ± 0.24 %ID/g (mean \pm SEM), in the control mouse tumor ($P = 0.0015$, Student t test; Fig. 5).

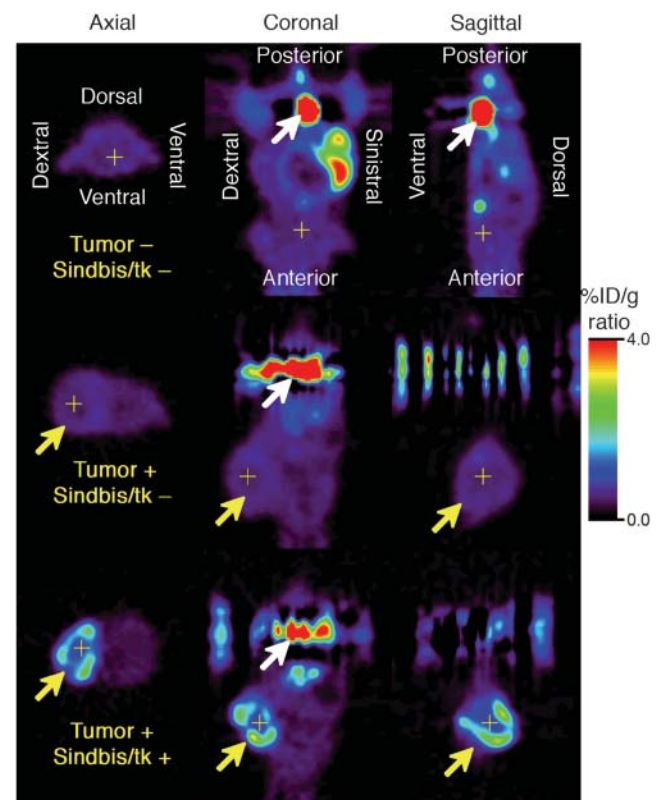


FIGURE 6. Noninvasive microPET of HSVtk activity in tumors after Sindbis/tk infection on day 14. BHK subcutaneous tumors were induced on right shoulders of SCID mice as indicated by yellow arrows. Tumor-bearing mice either received no vector treatment (Tumor +, Sindbis/tk -) or received 3 Sindbis/tk treatments via intraperitoneal injection far away from sites of tumor inoculation (Tumor +, Sindbis/tk +). Tumor-free control mice were also included to determine background signals caused by tracer retention within peritoneal cavity (Tumor -, Sindbis/tk -). HSVtk activity was determined after intravenous administration of ^{18}F -FEAU as tracer. Tomographic images are presented in axial, coronal, and sagittal views and crosshairs indicate triangulation points of the 3 views in each set of images. Coronal and sagittal images are shown with animal's head at bottom of image and white arrows indicate activity in urinary bladder. Signal intensity is presented in %ID/g.

Except for known routes of catabolism and excretion of ^{18}F -FEAU (Tumor -, Sindbis/tk -; Fig. 6) (27) through the liver, gallbladder, bladder, and gastrointestinal tract that were present in all animals imaged, the only site of focal radiotracer uptake was in the Sindbis/tk-transduced tumors.

DISCUSSION

In this particular study, using a combination of GCV treatment and quantitative PET, we provide proof-of-principle data for the use of the Sindbis viral vector system for GDEPT. The model tested is based on ES-2/Fluc cells derived from a clear cell ovarian carcinoma, known for its resistance to a variety of chemotherapeutic agents. Intraperitoneal inoculation of ES-2/Fluc cells in SCID mice induce an advanced disease characterized by rapid and widespread metastases within the peritoneal cavity. Our previous study indicated that the Sindbis vector, in the absence of any cytotoxic gene payload, is capable of systemic targeting and growth suppression of ES-2/Fluc tumor metastases (25). In the present study, we also observed a similar therapeutic effect of Sindbis/tk vector without the prodrug GCV (Fig. 3A). The vector alone achieved significant tumor growth suppression ($P = 0.0019$, 2-way ANOVA), which is largely attributed to the apoptotic nature of the Sindbis vector. Co-administration of GCV with Sindbis/tk treatments significantly enhances the therapeutic effectiveness of Sindbis/tk by taking advantage of the expression of HSVtk in Sindbis/tk-infected tumor cells (Fig. 3B). Activated GCV not only enhances the killing of the infected tumor cells but also causes bystander effects by transfer to the surrounding untransfected tumor cells. Because the infected tumor cells are doomed to an apoptotic fate regardless of the GCV treatment, the enhancement of the therapeutic efficacy of the Sindbis/tk vector is most likely due to the bystander effect, or a combination of both. In addition, the tumor apoptosis induced by Sindbis infection might enhance the bystander effects of GCV, as activated GCV could be transferred to surrounding tumor cells via apoptotic vesicles (28) in addition to gap junctions (19).

Beside a proper vector system, cancer GDEPT therapy would greatly benefit from a means to noninvasively monitor the GDEPT enzyme activity after vector treatments in vivo. Such capability could improve the Sindbis-based HSVtk/GCV GDEPT in clinical settings by providing important information to address 2 critical questions: (i) Do the vectors systemically target tumor cells and spare normal tissues? (ii) Do the tumors have sufficient expression levels of the enzyme for tumor eradication by subsequent prodrug activation? In addition, monitoring during the therapy could facilitate optimizing the dose and dosing schedule of the prodrug to reduce unwanted side effects.

Recent advances in optical and radionuclide imaging technology provide several methods for noninvasive monitoring of marker gene expression in living animals. Previously we have successfully detected tumor-specific targeting

of Sindbis vectors in small animals (6,25) using an optical bioluminescence imaging system. The advantages of bioluminescent imaging include short imaging time, low costs, and ease of use. However, optical imaging methods suffer from very substantial attenuation of the light signal and, thus, are not amenable to applications in large animals and in patients. On the other hand, radionuclide imaging methods such as γ -camera, SPECT, and PET have excellent depth sensitivity and can detect accumulation of gene expression within the transfected tumors anywhere in the body on the basis of gene expression imaging (22,29,30). A major advantage of PET is the ability to generate quantitative high-spatial resolution 3-dimensional images. When combined with other forms of tomographic imaging, such as CT or MRI, fusion images of functional and anatomic data will provide more detailed in situ information of marker genes' expression and localization.

For the purpose of gene expression imaging, several transgenes could provide promising payloads for Sindbis vector tumor-specific delivery in vivo, including the HSVtk, dopamine-2 receptor (31), or the sodium iodide symporter (32). For all of these systems, specific tumor targeting is rapid as is image contrast from clearance over time of the unreacted probe from normal tissues. For HSVtk, there are a variety of choices of reporter probes that may be used as well, both purine- and pyrimidine-based nucleosides, with varying radiotracer half-life, such as ^{18}F -FEAU (110-min half-life) and ^{124}I -FIAU (4-d half-life). FIAU labeled with ^{124}I , in particular, can be imaged several days after injection, at a time when virtually all of the unreacted tracer will have been cleared from the body and image contrast is maximized. A detailed comparison of the probes has been reported (33), and the pyrimidine-based tracers appear to have higher uptake than the purine ones. Also, the probe FIAU, when labeled with ^{124}I , can be imaged several days after injection, at a time when virtually all of the unreacted tracer will have been cleared from the body. Thus, the choice of probe will depend on the distribution of tumor and the time required to achieve effective tumor contrast for imaging.

In vivo transfection after parenteral administration of Sindbis vector appears to be very efficient, on the basis of a comparison of the percentage dose per gram uptake in the imaged tumors from the current study with reported uptake values in the literature (33). For example, after intravenous injection, FIAU uptake was 1.5 %ID/g, at 2 h after injection, in a tumor transfected in vitro (33), compared with our results (Fig. 6) of >3% dose per gram. Thus, in comparison with optimized in vitro transfection of tumor cells, there is a doubling of uptake after parenteral transfection of the Sindbis vector—this seems to us to be an indication of how efficient the biology of viral transfection can be in vivo under the right circumstances.

Thus, our data demonstrate the feasibility of detecting HSVtk enzyme activity in tumors after systemic treatment of a GDEPT vector in living animals. Our findings set the

stage for further exploration of currently available enzyme/prodrug combinations as a basis for developing different Sindbis-based GDEPT systems to achieve specific tumor detection, efficient prodrug activation, and accurate treatment evaluation.

CONCLUSION

In conclusion, the advantages of systemic tumor targeting and efficient transgene expression make Sindbis viral vector a promising agent for successful GDEPT. Using GDEPT and PET, it will be possible to explore currently available enzyme/prodrug combinations and develop different Sindbis-based GDEPT systems to achieve specific tumor detection, optimize efficient prodrug activation, and allow more accurate treatment planning and monitoring.

ACKNOWLEDGMENTS

This work was supported by National Institutes of Health Public Health Service grants CA22247, CA68498, CA100687, 5 P50 CA86438, R24 CA83084, 5 PO1 CA94060, and C06 RR11191; U.S. Army grant 0C000111; a grant from the Lustgarten Foundation; and a generous gift from the Karan-Weiss Foundation. We thank Dr. Christine Pampeno for her many comments and suggestions and for carefully reading this manuscript.

REFERENCES

1. Danks MK, Morton CL, Krull EJ, et al. Comparison of activation of CPT-11 by rabbit and human carboxylesterases for use in enzyme/prodrug therapy. *Clin Cancer Res.* 1999;5:917–924.
2. Austin EA, Huber BE. A first step in the development of gene therapy for colorectal carcinoma: cloning, sequencing, and expression of *Escherichia coli* cytosine deaminase. *Mol Pharmacol.* 1993;43:380–387.
3. Caruso M, Panis Y, Gagandeep S, Houssin D, Salzmann JL, Klatzmann D. Regression of established macroscopic liver metastases after *in situ* transduction of a suicide gene. *Proc Natl Acad Sci U S A.* 1993;90:7024–7028.
4. Serman DH, Treat J, Litzky LA, et al. Adenovirus-mediated herpes simplex virus thymidine kinase/ganciclovir gene therapy in patients with localized malignancy: results of a phase I clinical trial in malignant mesothelioma. *Hum Gene Ther.* 1998;9:1083–1092.
5. Greco O, Dachs GU. Gene directed enzyme/prodrug therapy of cancer: historical appraisal and future perspectives. *J Cell Physiol.* 2001;187:22–36.
6. Tseng JC, Levin B, Hirano T, Yee H, Pampeno C, Meruelo D. *In vivo* antitumor activity of sindbis viral vectors. *J Natl Cancer Inst.* 2002;94:1790–1802.
7. Tseng JC, Levin B, Hurtado A, et al. Systemic tumor targeting and killing by Sindbis viral vectors. *Nat Biotechnol.* 2004;22:70–77.
8. Wang KS, Kuhn RJ, Strauss EG, Ou S, Strauss JH. High-affinity laminin receptor is a receptor for Sindbis virus in mammalian cells. *J Virol.* 1992;66:4992–5001.
9. Liebman JM, Burbelo PD, Yamada Y, Fridman R, Kleinman HK. Altered expression of basement-membrane components and collagenases in ascitic xenografts of OVCAR-3 ovarian cancer cells. *Int J Cancer.* 1993;55:102–109.
10. Ozaki I, Yamamoto K, Mizuta T, et al. Differential expression of laminin receptors in human hepatocellular carcinoma. *Gut.* 1998;43:837–842.
11. Sanjuan X, Fernandez PL, Miquel R, et al. Overexpression of the 67-kD laminin receptor correlates with tumour progression in human colorectal carcinoma. *J Pathol.* 1996;179:376–380.
12. van den Brule FA, Berchuck A, Bast RC, et al. Differential expression of the 67-kD laminin receptor and 31-kD human laminin-binding protein in human ovarian carcinomas. *Eur J Cancer.* 1994;30A:1096–1099.
13. Balachandran S, Roberts PC, Kipperman T, et al. Alpha/beta interferons potentiate virus-induced apoptosis through activation of the FADD/caspase-8 death signaling pathway. *J Virol.* 2000;74:1513–1523.
14. Levine B, Huang Q, Isaacs JT, Reed JC, Griffin DE, Hardwick JM. Conversion of lytic to persistent alphavirus infection by the bcl-2 cellular oncogene. *Nature.* 1993;361:739–742.
15. Zrachia A, Dobroslav M, Blass M, et al. Infection of glioma cells with Sindbis virus induces selective activation and tyrosine phosphorylation of protein kinase C delta: implications for Sindbis virus-induced apoptosis. *J Biol Chem.* 2002;277:23693–23701.
16. Mar EC, Chiou JF, Cheng YC, Huang ES. Human cytomegalovirus-induced DNA polymerase and its interaction with the triphosphates of 1-(2'-deoxy-2'-fluoro-beta-D-arabinofuranosyl)-5-methyluracil, -5-iodocytosine, and -5-methylcytosine. *J Virol.* 1985;56:846–851.
17. Beltinger C, Fulda S, Kammertoens T, Meyer E, Uckert W, Debatin KM. Herpes simplex virus thymidine kinase/ganciclovir-induced apoptosis involves ligand-independent death receptor aggregation and activation of caspases. *Proc Natl Acad Sci U S A.* 1999;96:8699–8704.
18. Beltinger C, Fulda S, Kammertoens T, Uckert W, Debatin KM. Mitochondrial amplification of death signals determines thymidine kinase/ganciclovir-triggered activation of apoptosis. *Cancer Res.* 2000;60:3212–3217.
19. Dilber MS, Abedi MR, Christensson B, et al. Gap junctions promote the bystander effect of herpes simplex virus thymidine kinase *in vivo*. *Cancer Res.* 1997;57:1523–1528.
20. Gambhir SS, Barrio JR, Wu L, et al. Imaging of adenoviral-directed herpes simplex virus type 1 thymidine kinase reporter gene expression in mice with radiolabeled ganciclovir. *J Nucl Med.* 1998;39:2003–2011.
21. Hackman T, Doubrovin M, Balatoni J, et al. Imaging expression of cytosine deaminase-herpes virus thymidine kinase fusion gene (CD/TK) expression with [¹²⁴I]FIAU and PET. *Mol Imaging.* 2002;1:36–42.
22. Serganova I, Doubrovin M, Vider J, et al. Molecular imaging of temporal dynamics and spatial heterogeneity of hypoxia-inducible factor-1 signal transduction activity in tumors in living mice. *Cancer Res.* 2004;64:6101–6108.
23. Tjuvajev JG, Finn R, Watanabe K, et al. Noninvasive imaging of herpes virus thymidine kinase gene transfer and expression: a potential method for monitoring clinical gene therapy. *Cancer Res.* 1996;56:4087–4095.
24. Chatziioannou AF, Cherry SR, Shao Y, et al. Performance evaluation of microPET: a high-resolution lutetium oxyorthosilicate PET scanner for animal imaging. *J Nucl Med.* 1999;40:1164–1175.
25. Tseng JC, Hurtado A, Yee H, et al. Using sindbis viral vectors for specific detection and suppression of advanced ovarian cancer in animal models. *Cancer Res.* 2004;64:6684–6692.
26. Iijima Y, Ohno K, Ikeda H, Sawai K, Levin B, Meruelo D. Cell-specific targeting of a thymidine kinase/ganciclovir gene therapy system using a recombinant Sindbis virus vector. *Int J Cancer.* 1999;80:110–118.
27. Kong XB, Vidal P, Tong WP, Chiang J, Gloff CA, Chou TC. Preclinical pharmacology and pharmacokinetics of the anti-hepatitis virus agent 2'-fluoro-5-ethyl-1-beta-D-arabinofuranosyluracil in mice and rats. *Antimicrob Agents Chemother.* 1992;36:1472–1477.
28. Freeman SM, Abboud CN, Whartenby KA, et al. The “bystander effect”: tumor regression when a fraction of the tumor mass is genetically modified. *Cancer Res.* 1993;53:5274–5283.
29. Blasberg RG, Gelovani J. Molecular-genetic imaging: a nuclear medicine-based perspective. *Mol Imaging.* 2002;1:280–300.
30. Wen B, Burgman P, Zanzonico P, et al. A preclinical model for noninvasive imaging of hypoxia-induced gene expression: comparison with an exogenous marker of tumor hypoxia. *Eur J Nucl Med Mol Imaging.* 2004;31:1530–1538.
31. Yaghoubi SS, Wu L, Liang Q, et al. Direct correlation between positron emission tomographic images of two reporter genes delivered by two distinct adenoviral vectors. *Gene Ther.* 2001;8:1072–1080.
32. Dingli D, Russell SJ, Morris JC 3rd. *In vivo* imaging and tumor therapy with the sodium iodide symporter. *J Cell Biochem.* 2003;90:1079–1086.
33. Tjuvajev JG, Doubrovin M, Akhurst T, et al. Comparison of radiolabeled nucleoside probes (FIAU, FHBG, and FHPG) for PET imaging of HSV1-tk gene expression. *J Nucl Med.* 2002;43:1072–1083.